1. Slavomír LIPÁR, 2. Pavol NOGA, 3. Gabriel HULKÓ

MODELING AND CONTROL OF TEMPERATURE FIELD IN EXTRUSION AS DISTRIBUTED PARAMETER SYSTEM

1-3. Institute of Automation, Measurement and Applied Informatics, Faculty of Mechanical Engineering, Slovak University of Technology, Nám. slobody 17, 812 31 Bratislava, SLOVAKIA

Abstract: Modelling and control of the extruder temperature field is discussed, a process governed by a nonlinear partial differential equation. Utilizing finite element approximation a discretized input/output representation of the system is created with the inputs being powers of heaters and output the extruder temperature field. Local linearization is applied at the operating point and the controller is designed based on the lumped-input and distributed-parameter-output systems approach, using the time-space decoupling of system's dynamics
Keywords: extruder temperature, finite element, nonlinear partial differential equation

1. INTRODUCTION

Extrusion is the most common plastics and rubber processing technology. It is being used to pre-process the plastic mixture for subsequent operations (e.g. injection moulding and blow moulding) as well as for the production of finished profiles. The corresponding device is called an extruder. Several configurations are known, most commonly single- and twin-screw extruders with various modifications and enhancements, [1].

This paper deals with the control of a single screw extruder barrel temperature control. The barrel temperature field has a major influence on the product quality as well as the process itself. To get a closer insight to the problem, an experimental rig was built, Fig. 1a.
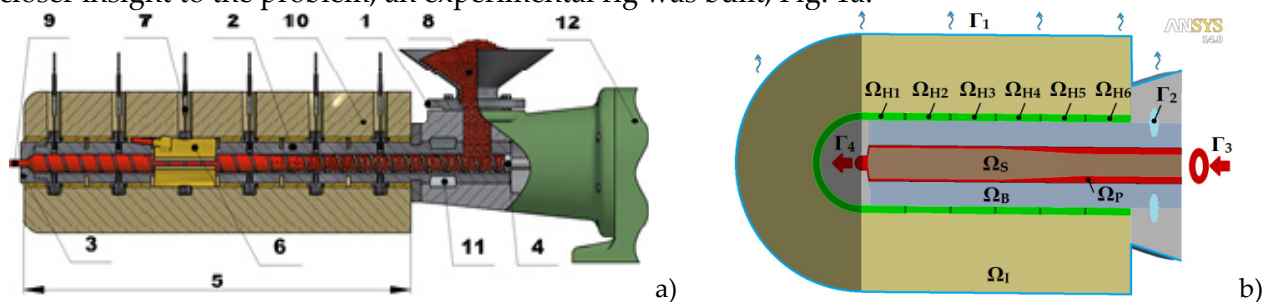
Figure 1. a) Extruder assembly: 1 – Hopper, 2 – Barrel, 3 – Die, 4 – Screw, 5 – Heated part, 6 – Heater band, 7 – Temperature probe, 8 – Material feed, 9 – Extruded profile, 10 – Insulation, 11 – Cooling channel, 12– Screw drive motor. b) Computational model.

The barrel's heated part (Fig. 1a. item 5) is subdivided into 6 zones, each having a heater band and temperature probe in order to control the temperature profile, which depends on the particular material being processed as well as the desired extruded profile and/or subsequent operations, [2]. Higher temperatures may be beneficial in order to facilitate material flow in the barrel and lowering production costs, however though, overheating results in too soft output material, or worse, rendering it useless due to irreversible heat induced degradation.

Regarding the temperature profile, most works focus on the melt exit temperature only and temperatures in the remaining zones are set relatively to this value as in [3], and [4]. In [3] the temperature in each zone is controlled individually by means of identical SISO PID controllers. In the presented work we use a similar structure, but with the SISO controllers interlinked via the Space Synthesis block, [6], so including into each individual control action computation the effect of all other zones as well.

As stated, the barrel temperature field is created by heater bands and monitored using temperature probes. The barrel-plastic-screw system is governed by a nonlinear partial differential equation (PDE). Modelling of this process was done by finite element method (FEM) using ANSYS Polyflow and the model validated on the laboratory rig. Control synthesis was performed on a linearized interval around the operating point and the loop set up using DPS Blockset by [7].

The paper is organized as follows. Section 2 describes the mathematical model of the barrel temperature control process, section 3 introduces the time-space decoupling based on the lumped input and distributed output (LDS) approach by [5] and [6], and finally section 4 displays the results.

2. MATHEMATICAL MODEL

We developed a simplified model of the extrusion process focused on the relation between the heater inputs and barrel temperature field. Since the model is used to estimate only temperatures and heat flux, the screw rotation and rheology of the extruded plastic are not considered. The PDE governing this system:

$$\rho c \left(\partial T / \partial t + \nabla T \cdot \mathbf{v} \right) - \nabla \cdot \left(\lambda \nabla T \right) = \dot{q}, \tag{1}$$

where T (K) is the temperature, $\dot{q}$ (W) heat sources/sinks, ρ (kg·m^{-3}) density, c (J·kg^{-1}·K^{-1}) specific heat, λ (W·m^{-1}·K^{-1}) thermal conductivity, $\mathbf{v}$ (m·s^{-1}) flow velocity.

The computational model, Fig. 1b, comprises the domains Ω_B – the barrel, Ω_P – the plastic, Ω_S – the screw, Ω_I – thermal insulation, and $\Omega_{H1\ldots6}$ – the heater bands; further the boundaries: Γ_1 – the outer surface, Γ_2 – the drive protection cooling channel, Γ_3 – cold plastic inlet, and Γ_4 – the hot plastic outlet.

2.1 Computational domains

The barrel and the screw are considered temperature invariant, thus linear in parameters, with ρ=7750 kg·m^{-3}, c=450 J·kg^{-1}·K^{-1}, and λ=20 W·m^{-1}·K^{-1}. This is a valid assumption considering the fact that the operating temperature range (25 – 300°C) is quite narrow for the steel these parts are made of, and the mentioned properties do not change significantly. The same is assumed for the insulation, λ=0.2 W·m^{-1}·K^{-1}, ρ=18 kg·m^{-3}, and c=1000 J·kg^{-1}·K^{-1}.

The plastic being extruded is a nonlinear domain with all three parameters varying with temperature, the main contribution being due to the phase change the plastic is undergoing, Fig. 2. Latent heat of solidification is included in the heat capacity. Additionally, for computational simplicity, the plastic is considered an isotropic compressible non-viscous fluid throughout the whole temperature range (including phase change in the real material) entering the barrel at the hopper side and leaving through the die.
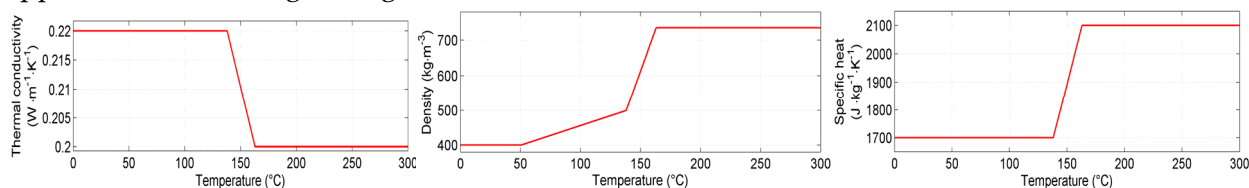
Figure 2. Parameters of the extruded plastic

Heater bands are six linear domains serving basically only the heat input generation. This is generated in the heater bands by electric resistance heating, which is controlled by thyristorsfor each channel separately. Joule's law states

$$Q_{el} = R I^2 t = P_{el} t, \tag{2}$$

where R (Ω) is resistance, I (A) current, P_{el} (W) electric power. The input heat generated in the heater band (per unit volume) is

$$\dot{q}_{Hi} = Q_{el,i}/(t V_{Hi})\big|_{i=1...6} = P_{el,i}/V_{Hi}\big|_{i=1...6}, \tag{3}$$

where V_{Hi} (m^3) is the i-th heater band volume. This heat is being transferred via domain interfaces predominantly to the barrel, just a minor part dissipates to the surroundings thanks to the insulation.

2.2 Boundary conditions

The extruder outer surface is subject to free air cooling.

$$\dot{q}(\mathbf{x},t) = h(T(\mathbf{x},t) - T_A), \quad \mathbf{x} \in \Gamma_1, \tag{4}$$

where $\mathbf{x}=(x,y,z)$ is the spatial coordinate, h (W·m^{-2}·K^{-1}) the convection heat transfer coefficient, T_A=25°C temperature of the surrounding air. For the operating temperature range the effect of radiation may be neglected, or better, can be easily linearized by including it in the convection heat transfer coefficient,[8].

Barrel cold-end cooling is incorporated in form of a Dirichlet boundary condition with the surface temperature T_W=15°C.

$$T(\mathbf{x},t) = T_W, \quad \mathbf{x} \in \Gamma_2. \tag{5}$$

Plastic inlet Γ_3 has a defined mass flow rate Q_m (kg·s^{-1}) and inflow temperature T_{in}=25°C.

$$T(\mathbf{x},t) = T_{in}, \quad \mathbf{v}(\mathbf{x},t) = Q_m/(\rho(\mathbf{x},T) S_{\Gamma3}), \quad \mathbf{x} \in \Gamma_3, \tag{6}$$

where $S_{\Gamma3}$ (m^2) is the inlet cross-section surface.

The mass conservation law requires the in- and outflow rate being equal, therefore the flow velocity is changing with fluid density throughout the domain. So the plastic outlet boundary condition is as follows

$$\mathbf{v}(\mathbf{x},t) = Q_m/(\rho(\mathbf{x},T) S_{\Gamma4}), \quad \mathbf{x} \in \Gamma_4, \tag{7}$$

where $S_{\Gamma4}$ (m^2) is the outlet cross-section surface. Amount of heat extracted from the system is driven by the plastic flow rate and outlet temperature at the die. This model was discretized by FEM with a tetragonal mesh using ANSYS and the FEM model then validated experimentally on the rig, Fig. 3b.

3. CONTROLLER DESIGN

The extruder barrel temperature field, a spatially distributed quantity, is controlled by 6 individual heater bands, whose inputs are electric currents, lumped quantities. Such a system in general is referred to as a lumped-input and distributed-parameter-output system (LDS).
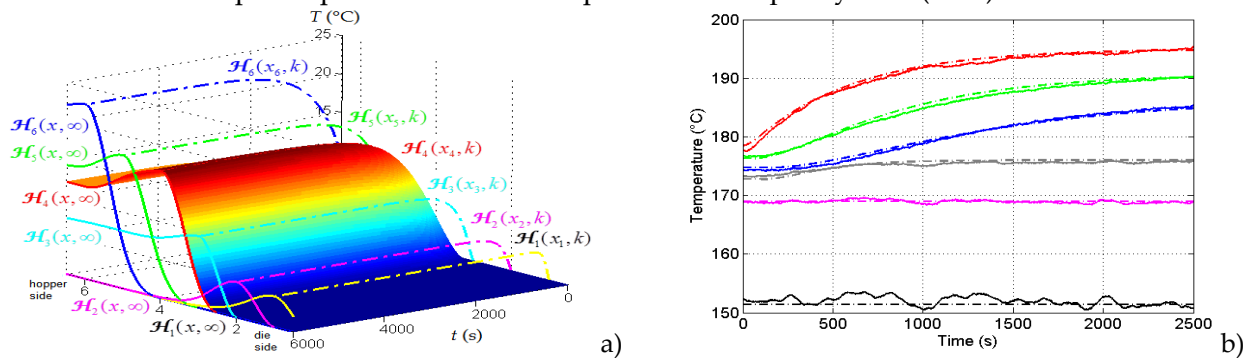
Figure 3. a) Extruder barrel temperature field step responses. b) Response of the system to a step change in power of heater #4, simulated (dashed) and measured (solid).

Being in neighbourhood of the operating point of our concern, the locally linearized system output can be expressed as the sum of effects of all control variables (the discrete case is considered in the following).

$$Y(\mathbf{x},k) = \sum_{i=1}^{6} Y_i(\mathbf{x},k) = \sum_{i=1}^{6}\sum_{q=0}^{k} \mathcal{G}_i(\mathbf{x},q)U_i(k-q), \tag{8}$$

where $Y(\mathbf{x},k)$ is the system output, $Y_i(\mathbf{x},k)$ i-th output component (effect of the i-th actuator), $\mathbf{G}_i(\mathbf{x},k)$ corresponding impulse responses of the system, U_i i-th control variable, k time step. Impulse responses can be either are calculated from the step responses $\mathbf{H}_i(\mathbf{x},k)$, which are either measured or estimated by a computational model as in our case.

$$\left\{\mathcal{G}_i\left(\mathbf{x},k\right)=\mathcal{H}_i\left(\mathbf{x},k\right)-\mathcal{H}_i\left(\mathbf{x},k-1\right)\right\}_{i=1\ldots6}. \tag{9}$$

Further in the text we will work with a length coordinate only (replacing $\mathbf{x}$ by x in the equations) since our interest lies in the temperature profile along the barrel which is rotationally symmetrical.

A closer look at the step responses, Fig. 3a., reveals the crucial fact, that each one has a point where the response is most intensive., the maximum gain point. This response is called the partial step response (the maximum gain response) $\mathbf{H}_i(x_i,k)$, where x_i is the maximum gain point for the i-th input.

Measurements performed on the real system are preferably taken from the proximity of these maximum gain points, which are generally closest to the actuator. The partial impulse responses $\mathbf{G}_i(x_i,k)$ follow from (9) and the corresponding transfer functions $\{S_i(z)\}_{i=1\ldots6}$. are assigned.

$$Y_i\left(x_i,k\right)=S_i\left(z\right)U_i\left(k\right), \tag{10}$$

where $\{Y_i(x_i,k)\}_{i,k}$ are partial outputs in highest-gain points. These will represent time components of the system's dynamics. Furthermore, we introduce the normalized partial impulse responses in space domain, which represent the system's dynamics in space.

$$\left\{\mathcal{G}R_i\left(x,k\right)\right\}_{i,k}=\left\{\mathcal{G}_i\left(x,k\right)\big/\mathcal{G}_i\left(x_i,k\right)\right\}_{i,k}, \tag{11}$$

for $\mathbf{G}_i(x_i,k)\neq0$. Then the system output can be expressed as

$$Y\left(x,k\right)=\sum_{i=1}^{6}\sum_{q=0}^{k}\mathcal{G}_i\left(x_i,q\right)\mathcal{G}R_i\left(x,q\right)U_i\left(k-q\right). \tag{12}$$

Analogously, for the steady states $\mathbf{H}_i(x,\infty)$ we introduce the normalized steady-state values

$$\left\{\mathcal{H}R_i\left(x\right)\right\}_{i,k}=\left\{\mathcal{H}_i\left(x,\infty\right)\big/\mathcal{H}_i\left(x_i,\infty\right)\right\}_{i,k}, \tag{13}$$

where $\{\mathbf{H}_i(x_i,\infty)\neq0\}_{i=1\ldots6}$ are steady state values in the highest-gain points.

The system's steady-state output becomes

$$Y\left(x,\infty\right)=\sum_{i=1}^{6}Y_i\left(x_i,\infty\right)\mathcal{H}R_i\left(x\right), \tag{14}$$

Once the system's dynamics is decomposed into time-domain characteristics $\{\mathbf{G}_i(x_i,k)\}_{i=1\ldots6}$, $\{S_i(z)\}_{i=1\ldots6}$ and space-domain characteristics $\{\mathbf{G}R_i(\mathbf{x},k)\}_{i=1\ldots6}$, $\{\mathbf{H}R_i(\mathbf{x})\}_{i=1\ldots6}$, the control problem can be split into space-domain and time-domain problems. Fig. 4a shows the control loop arrangement.

3.1 Space and time-domain control synthesis

Based on (14), the output/state of the controlled system is expressed as a weighted sum of partial distributed-parameter responses. In fact, these weights express the contribution of each actuating member to the overall output/state.
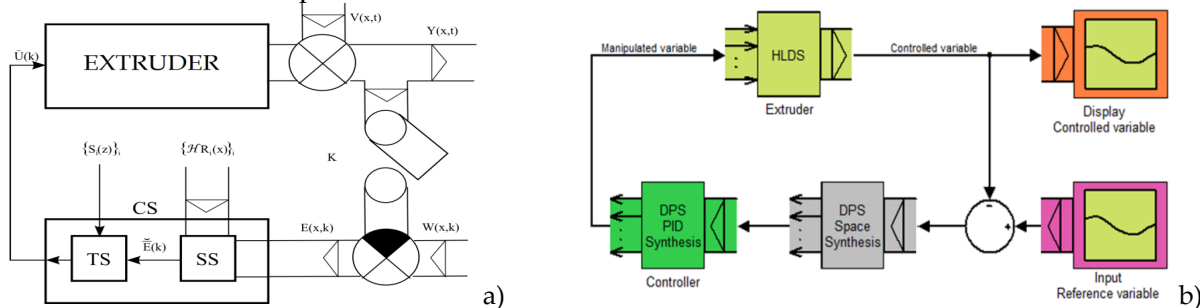
Figure 4. a) Feedback control loop. CS – control system, TS/SS – time/space domain synthesis, K – time/space sampling, W(x,k) – desired temperature profile, E(x,k) – distributed control error, Ē(k) vector of transformed control errors, V(x,k) – disturbance, Ū(k)={U_i(k)}_{i=1...6} – vector of lumped control quantities. b) Control loop using DPS Blockset.

The Space Synthesis block solves optimal approximation of the system's output, reference or control error, depending on the control loop configuration, on the system's distributed parameter output space (a strictly normed function space) with the base $\{\mathbf{H}R_i(\mathbf{x})\}_{i=1\ldots6}$.

$$\left\{\breve{E}_i\left(k\right)\right\}_i = \arg\min_{\left\{\breve{E}_i(k)\right\}_i}\left\|E\left(x,k\right)-\sum_{i=1}^{6}\breve{E}_i\left(k\right)\mathcal{H}R_i\left(x\right)\right\|, \tag{15}$$

thus finding the optimal approximation coefficients, which is a transformation of the distributed control error to a vector of lumped quantities. This transformed control error is processed by the time domain controller.

The control problem is solved in time domain by means of a group of SISO regulators, $\left\{R_i\left(z\right)\right\}_i$, which are tuned to the time components of the system's dynamics $\{\mathbf{G}_i(\mathbf{x}_i,k)\}_{i=1\ldots6}$ or the corresponding transfer functions $\{S_i(z)\}_{i=1\ldots6}$.

Using this approach the control problem is reduced to a group of SISO control problems, since the individual controllers are tracking the transformed quantities, instead of solving a full-scale DPS optimization problem or a MIMO controller synthesis. This enables to use any control synthesis approach developed for SISO systems, without the need of special adaptation to DPS.

3.2 Controllability in space

Number and location of actuating members and measurement points, if not fixed in advance by the technology, is to be carefully chosen depending on the nature of the process. In order to make the control problem solution feasible in space-domain, the following must hold:

$$\left\|W\left(x\right)-\sum_{i=1}^{6}Y_i\left(x_i,\infty\right)\mathcal{H}R_i\left(x\right)\right\| \leq \delta, \tag{16}$$

where δ is the tolerance given by the technology. This condition becomes more stringent with the increasing number of measuring points. In case of a square plant (as our case) this depends solely on the values in highest gain points.

In the experimental rig (let us recall Fig. 1a.), for each zone we have one temperature probe for monitoring. They are located in the barrel walls 10mm from inner surface. It is obvious that their location in the highest gain points is the optimal one (we observe the barrel temperature along the line where these are located). In general, number of probes should be at least the number of actuators for the control problem (15) to be determinate, as it is in our case. In this way, the control synthesis (16) is performed on a reduced domain taking the system output at the measuring points $\{x_{1\ldots6}\}\subset\Omega$, i.e. solving the problem on a subset of the whole definition domain Ω. If the reference variable $\mathbf{W}_{nFull}$ is given on the full domain, the equivalent reference values $\mathbf{W}_{nRed}$ for the reduced domain is calculated by

$$\mathbf{W}_{nRed} = \mathcal{H}R_{nRed}\mathcal{H}R_{nFull}^{+}\mathbf{W}_{nFull}, \tag{17}$$

where $\mathbf{H}R_{nRed}$ are reduced domain steady-states and $\mathbf{H}R_{nRed}$ are full domain steady states (all quantities already discretized and in matrix form). This ensures that the solution of control problem (15) will be the same in the full domain cases as well as in the reduced domain case, which enables to reduce computational load and memory requirements by reducing the plant to the minimum configuration – a square plant with number of outputs equal to the number of inputs. The full scale effect however is still preserved being determined by the plant's distributed nature.

The (reduced domain) control loop was set up in MATLAB-Simulink using DPS Blockset, Fig. 4b. In time domain PID controllers with anti-windup were used.

4. RESULTS

A set-point change was considered. The nonlinear nature of the plastic, especially the changing density and heat capacity cause shifts in the heat extraction by the output material not only in the output zone, but having effect on the whole temperature field. The challenging part is that the extruded profile is expected to be at a temperature, where it is holding its shape. This means being close to the solid/liquid interface where nonlinearities are the strongest.

Feedback control was applied to the FEM model described in section 2 of this paper. The control process is shown in Fig. 5a. As can be seen from the control actions, Fig. 5b, a significant load disturbance is not present. This is due to the extruder construction and the resulting relatively high inertia of the system. Another factor is the extruded material. It is assumed and desired to process one quality at a time. The feed material has usually very low variation in composition, consequently also in thermal properties, thus not causing fluctuations in heat fluxes. Set-point changes are usually induced by subsequent processing units.
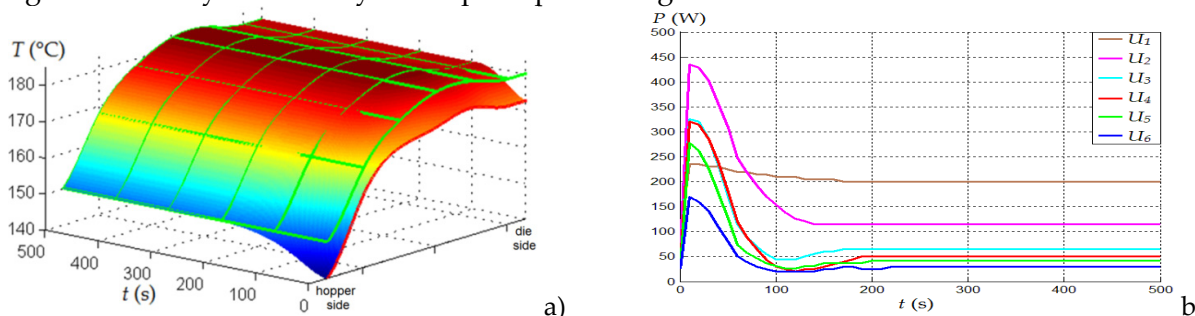
Fig. 5. a) Barrel temperature field control process. Red line– old set-point (and steady state); Green line – new set-point. b) Control actions (electrical power inputs to heaters).

5. CONCLUSIONS

We presented the design of a numerical model of an extruder barrel including plastic flow and the related control system. The model was created using ANSYS Polyflow and validated experimentally. This model serves as a generator of extruder characteristics at various set-points to which the controller is tuned. Features and capabilities of FEM software packages for various technologies are still not exploited enough in DPS control synthesis problems. The authors' works also aim to facilitate this matter.

The proposed control system for the barrel temperature field control, a nonlinear process, is based on the LDS approach using local linearization. By this approach the system set-up is very straightforward with low requirements on controller hardware, software as well as operator knowledge, making it suitable for industrial application.

REFERENCES
[1.] Rauvendaal, C. (2001). Polymer extrusion, 4th edition, Hanser Verlag, München.
[2.] Harold, F.G., Wagner, J.R., and Mount, E.M. (2005). Extrusion: The definitive processing guide and handbook, Wiliam Andrew Inc., Norwich.
[3.] Previdi, F., Savaresi, S.M., Panarotto, A. (2006). Design of a feedback control system for real-time control of flow in a single-screw extruder. Control engineering practice, vol. 14, pp. 1111–1121.
[4.] Garge, S.C., Wetzel, M.D., Ogunnaike, B.A. (2012). Control-relevant model identification of reactive extrusion processes. Journal of process control, vol. 22, pp. 1457–1467.
[5.] Hulkó, G. et al. (1998). Modeling, control and design of distributed parameter systems with demonstrations in MATLAB. Publishing house of STU, Bratislava.
[6.] Hulkó, G. et al. (2009). Engineering methods and software support for modelling and design of discrete-time control of distributed parameter systems. European journal of control, vol. 15, (no. 3–4), pp. 55–73.
[7.] Hulkó G. et al. (2003-2012) Distributed Parameter Systems Blockset for MATLAB & Simulink – Third-Party Product of The MathWorks. Publishing house of STU, Bratislava.
[8.] Zhang, B., Maijer, D.M., and Cockroft, S.L. (2007). Development of a 3-D thermal model of the low-pressure die-cast (LPDC) process of A356 aluminum alloy wheels. Materials science and engineering A, vol. 464, pp. 295–305.